The Geometry and Size Dependence of the Common Format Constraint Factor

J.R. Donoso[1], U. Muehlich[1], and J.D. Landes[2]

[1] Materials Science Department, Universidad Santa María, Valparaíso, CHILE
[2] MAES Department, The University of Tennessee, Knoxville, TN, USA.

ABSTRACT: *This paper addresses the behavior of the Common Format Equation (CFE) constraint factor Ω^*, for C(T), SE(B), and M(T) specimens. Values of Ω^* are obtained from numerical data for these three geometries as a function of the size parameter B/b, i.e., the thickness-to-ligament ratio. The results indicate a geometry- and size-dependence of the constraint factor in the range of B/b employed, roughly from 0.15 to little less than 4.0. The C(T) and SE(B) specimens show a smooth transition of their Ω^* values from plane strain to plane stress in the whole B/b range. In the same range, the M(T) specimens show much lower Ω^* values. One clear consequence for the M(T) geometry is that it may never reach a plane strain state, as defined by the CFE, when compared to C(T) and SE(B) specimens.*

INTRODUCTION

The constraint issue has been extensively studied for its significance in Fracture Mechanics. In fact, fracture toughness, given by the J-R curve, is strongly dependent on planar specimen dimensions, loading mode, and crack length. The constraint not only affects the fracture toughness of a material, but the load-displacement relations (i.e., the calibration functions) are also affected by the degree of constraint of the cracked specimen or component. As has been shown [1], the constraint influences the fracture properties and the calibration functions in opposite ways. A plane strain condition lowers the J-R curve and raises the load-displacement curve of the specimen. Conversely, a plane stress condition raises the J-R curve and lowers the corresponding load-displacement curve. The fracture toughness evaluations according to test standards require a plane strain condition, that is, demands testing highly constrained specimens [2].

In a ductile fracture methodology, both the fracture toughness as well as the calibration functions are needed. So far, the emphasis has been placed on evaluating the fracture toughness behavior rather than on determining the load-displacement relation of a cracked component. Donoso and Landes

filled the gap in this subject with the development of the Common Format Equation, CFE [3,4]. In fact, the CFE calibration functions, which relate load with crack length and plastic displacement, give a good description of the load-plastic displacement behavior of notched or cracked components. The CFE includes a constraint factor Ω* which has been used to evaluate the relative constraint of the specimen, as will be shown next.

THE COMMON FORMAT CONSTRAINT FACTOR Ω*

In the CFE approach [3] the load, P, is expressed as the product of three terms, as shown by Equation (1):

$$P = \Omega^* \cdot G\left(\frac{b}{W}\right) \cdot H\left(\frac{v_{pl}}{W}\right) \qquad (1)$$

In Equation (1), G is a geometry, ligament size-dependent function; H is a hardening function, and Ω* is the CFE constraint factor. The functions G and H are well known, and have been discussed elsewhere [4]. Evaluation and/or prediction of the CFE constraint factor Ω*, on the other hand, have always been a difficult task. Even though the degree of constraint influences both the fracture toughness evaluations as well as the load-displacement relations, one can say that Ω*, the Common Format Equation deformation-based constraint parameter is, in many cases, completely ignored.

The two-dimensional approach to the in-plane constraint problem gives two values for the constraint factor. Thus, planar fracture specimens display a 2-D behavior which is either plane strain or plane stress. Consequently, the constraint factor of Eq. (1) attains a specific value: in the CFE approach, Ω* is equal to 0.3638 (1.455/4) for pure plane strain behavior, and 0.2678 (1.071/4) for plane stress [1,3]. For 3-D specimens, both experimental and numerical evidence show that values of Ω* in between are possible, which would indicate a tendency for the behavior of the specimen, depending on type of specimen (geometry), loading conditions (tension vs. bending), planar dimensions (crack length and width), and specimen thickness [5].

In the initial work of Donoso and Landes, a map of constraint behavior was constructed, giving Ω* as a function of the specimen thickness-to-ligament ratio of C(T) specimens of various thickness and planar dimensions [1]. Thus, it was possible to identify the size requirements for the specimen to behave in plane strain or in plane stress. No attempt was made then to look into the significance of Ω* values in between the two

extreme values of 0.2678 and 0.3638. In that work, the method proposed by Donoso and Landes for the evaluation of the degree of constraint consisted in examining the normalized load – normalized displacement relationship based on a power law type of equation for H, as shown in Equation (2):

$$P_N = \frac{P}{G} = \Omega^* \sigma^* v_N^{1/n} = D\, v_N^{1/n} \tag{2}$$

In Equation (2), v_N, the normalized displacement, is v_{pl}/W, and G, the geometry function, also follows a power law dependence on the normalized ligament, b/W, of the type $G = C \cdot B \cdot W \cdot (b/W)^m$, in which B is the specimen thickness, W is a typical specimen dimension (width), b is equal to W – a, where a is crack length, and C and m are the CFE coefficient and exponent, respectively, characteristic of the geometry employed. Further analysis of the experimental or numerical load-displacement data in the format P_N versus v_N, gives the value of D, which is, in turn, equal to $\Omega^*\sigma^*$. Thus, the CFE constraint factor may be calculated through the knowledge of σ^*, if one starts from experimental P-v and stress-strain data [4].

An alternative way of calculating Ω^*, based upon numerical data (used throughout this work), is to make use of Eq. (1), and compare the P-v_{pl} data for 3-D specimens with those of 2-D specimens of the same crack length, a/W. This procedure has been explained elsewhere [5], and relies on the use of Eq. (1) for three situations, namely: a 2-D evaluation under plane strain (PSn) conditions; a 2-D evaluation under plane stress (PSs), and the 3-D evaluation. For a given set of material property and normalized crack length, Eq. (1) will read as follows for the three situations described:

$$P_u = (\Omega^*)_u \cdot G \cdot H(v_1) \tag{3}$$

$$P_{3\text{-}D} = (\Omega^*)_{3\text{-}D} \cdot G \cdot H(v_1) \tag{4}$$

$$P_l = (\Omega^*)_l \cdot G \cdot H(v_1) \tag{5}$$

where the subscript “u” stands for *upper* limit for Ω^* attained under plane strain (0.3638), “3-D” for the value of Ω^* for the 3-D case under analysis, and “l” for the *lower* limit of Ω^* under plane stress (0.2678).

The values of $(\Omega^*)_{3\text{-}D}$ are thus computed from the ratio of any two pairs of equations from (3) to (5), with Eq. (4) as the central pivotal term. Since G and H are the same for the chosen crack length and material, both will be cancelled. For example, taking Eqs. (4) and (5), the value of Ω^* will be:

$$(\Omega^*)_{3\text{-}D} = (P_{3\text{-}D} / P_l)\,(\Omega^*)_l = 0.2678\,(P_{3\text{-}D} / P_l) \qquad (6)$$

The constraint values for the M(T) specimen were defined in the EPRI Handbook as 1.0 for plane stress, and $2/\sqrt{3}$ for plane strain [6]. In order to compare these with the C(T) and SE(B) Ω^* values, the M(T) factors were corrected in such a way that the minimum constraint factor of 1.0, became the equivalent of 0.2678, and the ideal maximum, $2/\sqrt{3}$ became 0.3638. This correction was done with the following expression:

$$\frac{\Omega^* - 0.2678}{0.3638 - 0.2678} = \frac{(\Omega^*)_{3-D} - 1.0}{2\sqrt{3} - 1.0} \qquad (7)$$

in which $(\Omega^*)_{3\text{-}D}$ is obtained from Eq. (6), and Ω^* is the corrected value.

NUMERICAL ANALYSIS AND RESULTS

The load vs. plastic displacement data were numerically generated for the three geometry: C(T), SE(B), and M(T). A schematic is shown in Figure 1.

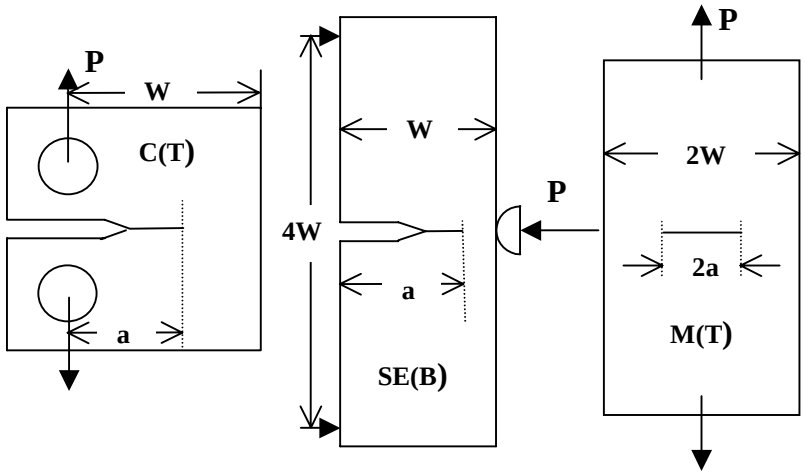

Figure 1.- Schematic planar view of the C(T), SE(B), and M(T) specimens.

In order to assure the existence of a wide range of Ω^* values, the C(T) and SE(B) specimens were constructed with various thickness, but their planar dimensions were fixed according to the recommendations of ASTM E1820 [2], proportional to B = 25 mm. Thus, all planar dimensions were the same (with the exception of crack length), whereas B was given values of 3.125, 6.25, 12.5, 18.75, and 25 mm. The M(T) specimen was given planar dimensions equivalent to two SE(B) specimens, i.e., 2Wx4W, with crack length 2a. The thickness of the various M(T) specimens were the same as the C(T) and SE(B) specimens.

Table 1 shows the normalized crack lengths employed (blunt-notch), and the thickness of the specimens analyzed. The result of this matrix is shown as B/b values where b, the ligament, is equal to W-a for all three geometries.

Not all 20 values of B/b in the matrix of Table 1 were used in this work. Some ratios are repeated (B/b = 0.42, or 0.83), and others are close enough to discard one or more of them (0.21 vs. 0.23 vs. 0.28). For C(T) and M(T), 11 B/b ratios were used, covering a wide range from 0.11 to 3.33, whereas only 7 B/b values within this range are reported for SE(B). The use of B/b as the main parameter for comparison has been explained elsewhere [5].

Table 1: B/b values for the specimens

a/W↓ | B, mm→	3.125	6.25	12.5	18.75	25
0.45	0.11	0.23	0.45	0.68	0.91
0.55	0.14	0.28	0.56	0.83	1.11
0.70	0.21	0.42	0.83	1.25	1.67
0.85	0.42	0.83	1.67	2.50	3.33

The ABAQUS [7] non-linear finite element code was employed to model the behavior of the three types of fracture test specimens. Due to the symmetry of the specimens shown in Figure 1, 3-D meshes consisting of one-fourth of the C(T) and SE(B) specimens, and one-eight of the M(T) specimen, were constructed. For the 2-D analysis, the specimen fractions used were ½, ½, and ¼, respectively. The mechanical properties used for the finite element calculations were the yield stress of the material, 240 MPa, and the power law stress-strain parameters, obtained from tensile tests conducted on ASTM A-516 Gr. 65 steel.

On the average, the 3-D models were constructed with 1200 8-node bricks, with a total of about 2500 nodes. The elements located around the crack tip were diminishing in size down to approximately 0.375 mm by 0.375 mm at the crack tip, which in turn was given a radius of curvature of 1 mm. The 2-D models, on the other hand, were similar to their 3-D counterparts in terms of planar sizes, but were constructed with 2-D elements. The calculation scheme used von Mises yield criterion, isotropic hardening and updated Lagrangian formulation. The 2-D specimens for each B/b value were analyzed under plane strain and plane stress conditions, in order to produce the information needed to obtain Ω^*, using Eq. (6), as explained earlier.

Figure 2 shows an example of the 2-D (upper, plane strain, and lower, plane stress) curves, with two 3-D curves in the middle, all for a/W = 0.70. Figure 3 shows the results for the constraint factor, as Ω^* vs. B/b curves.

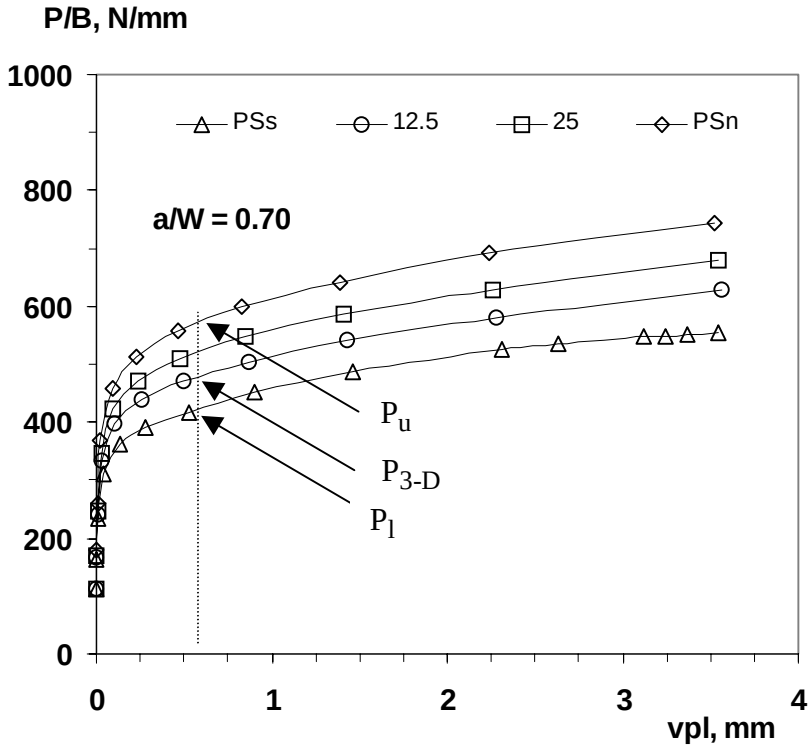

Figure 2.- Schematic of the procedure to evaluate Ω^* for the 3-D case.

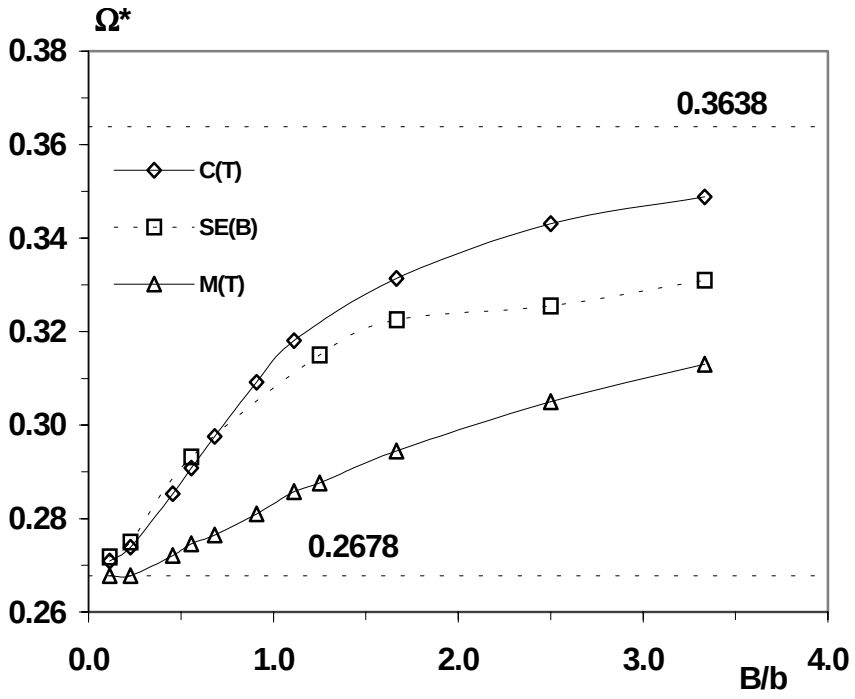

Figure 3.- Values of Ω* as a function of B/b.

DISCUSSION AND CONCLUSIONS

From the results shown in Figure 3, several conclusions may be drawn:

a) Ω* is close to the plane stress value for low B/b values. These "low" values seem to be slightly dependent on the geometry. The critical low value for C(T) and SE(B) is of the order of 0.1, whereas for M(T) is about 0.25.

b) Ω* shows a tendency towards the plane strain value for the C(T) geometry, at least for large B/b values. The attainment of plane strain also depends on geometry, and may never be reached by the M(T) geometry.

c) At any given B/b value, Ω* is the higher for the C(T), followed close by the SE(B) values (dashed curve), which show a sensitivity to the choice of v_{pl}. The M(T), on the other hand, is the lower of all. On examining the Ω* behavior going from high to low B/b values, one could say that the M(T) specimens show a dramatic drop in Ω* compared to C(T) and SE(B).

d) Since Ω^* depends solely on the B/b ratio [5], regardless of the specimen dimensions needed to obtain that ratio, then the size parameter B/b may be defined as "equivalent thickness".

The knowledge of Ω^* as a function of the equivalent thickness B/b should be helpful in fracture toughness testing. A C(T) specimen in a plane strain state may now be defined (arbitrarily) as having $B/b \geq 3$, where $\Omega^* \geq 0.35$. This means a number of combinations of thickness, B, and ligament, b (the latter given in a more practical manner as crack length, a). One combination would be a 1T C(T) specimen (B = 25 mm and all planar dimensions proportional to B as per ASTM E1820), with crack length $a/W \geq 0.83$. If this 1T C(T) specimen had only a/W = 0.7, hence B/b = 1.67, Ω^* would decrease to around 0.33.

The M(T) specimen, on the other hand, with $\Omega^* < 0.320$ in the range $B/b < 4.0$, may never reach a plane strain state, as has been defined and observed for C(T) and SE(B). The trend for M(T) shown in Figure 3, would indicate that the plane stress component of Ω^* is predominant in this geometry [5].

ACKNOWLEDGMENTS

The authors acknowledge the financial support from FONDECYT-Chile, research projects 1010151 and 7010151, and UTFSM-DGIP 210121.

REFERENCES

1. Donoso, J.R., and Landes, J.D., (1993) *Int. J. of Fracture*, 63, 275-285.
2. Standard Test Method For Measurement of Fracture Toughness, ASTM E 1820-99a, ASTM Annual Book Of Standards, vol. 03-01.
3. Donoso, J.R. and Landes, J.D., (1994) *Eng. Fract. Mech*., 47, 5, 619-628.
4. Donoso, J.R. and Landes, J.D., (1996) *Eng. Fract. Mech*., 54, 4, 499-512.
5. Donoso, J.R., Muehlich, U., Cancino, C. and Landes, J.D., (2001) submitted for publication.
6. Kumar, V., German, M.D., and Shih, C.F., EPRI NP-1931, July 1981.
7. Abaqus (2000) Version 6.1 Hibbitt, Karlsson and Sorensen, Pawtucket, R.I.